Available online at www.sciencedirect.com
SCIENCE DIRECT®
PERGAMON
Phytochemistry 63 (2003) 803–816
PHYTOCHEMISTRY
www.elsevier.com/locate/phytochem

Insecticidal pyrido[1,2-*a*]azepine alkaloids and related derivatives from *Stemona* species

Elisabeth Kaltenegger[a], Brigitte Brem[a], Kurt Mereiter[b], Hermann Kalchhauser[c,✝], Hanspeter Kählig[c], Otmar Hofer[c,*], Srumya Vajrodaya[d], Harald Greger[a,*]

[a]*Comparative & Ecological Phytochemistry Department, Institute of Botany, University of Vienna, Rennweg 14, A-1030 Vienna, Austria*
[b]*Department of Chemistry, Vienna University of Technology, Getreidemarkt 9/164SC, A-1060 Vienna, Austria*
[c]*Institute of Organic Chemistry, University of Vienna, Währingerstrasse 38, A-1090 Vienna, Austria*
[d]*Department of Botany, Faculty of Science, Kasetsart University, Bangkok 10900, Thailand*

Received 2 April 2003; received in revised form 9 May 2003

Abstract

Eight new alkaloids, the pyrido[1,2-*a*]azepines stemokerrin, methoxystemokerrin-*N*-oxide, oxystemokerrin, oxystemokerrin-*N*-oxide, and pyridostemin, along with the pyrrolo[1,2-*a*]azepines dehydroprotostemonine, oxyprotostemonine, and stemocochinin were isolated from four *Stemona* species together with the known compounds protostemonine, stemofoline, 2′-hydroxystemofoline, and parvistemonine. Their structures were elucidated by ^{1}H and ^{13}C NMR including 2D methods and two key compounds additionally by X-ray diffraction. Besides the formation of a six membered piperidine ring, additional oxygen bridges and *N*-oxides contributed to structural diversity. The co-occurrence of pyrrolo- and pyridoazepines suggested biosynthetic connections starting from more widespread protostemonine type precursors. Bioassays with lipophilic crude extracts against *Spodoptera littoralis* displayed very strong insecticidal activity for the roots of *S. curtisii* and *S. cochinchinensis*, moderate activity for *S. kerrii*, but only weak effects for the unidentified species HG 915. The insect toxicity was mainly caused by the accumulation of stemofoline, oxystemokerrin, and dehydroprotostemonine displaying two different modes of action. Based on the various insecticidal activities of 13 derivatives structure–activity relationships became apparent.

Keywords: *Stemona kerrii*; *S. curtisii*; *S. cochinchinensis*; *S.* species indet.; Stemonaceae; *Stemona* alkaloids; Pyrrolo[1,2-*a*]azepines; Pyrido[1,2-*a*]-azepines; *Spodoptera littoralis*; Insect toxicity; Structure–activity relationships

1. Introduction

Stemona comprises about 25 species and represents the largest genus of the small monocotyledonous family Stemonaceae. Many species prefer a seasonal climate and occur as perennial climbers or subshrubs with tufted tuberous roots in rather dry vegetation ranging from continental Asia and Japan through Southeast Asia to tropical Australia. In spite of the good delimitation of *Stemona* from the nearest related genera *Croomia* and *Stichoneuron* and already existing more recent revisionary treatments for the Flora Malesiana (Duyfjes, 1993) and China (Tsi and Duyfjes, 2000), there are still many taxonomic problems at the species level that remain to be solved. Since the roots of several species are widely used as insecticides and for medicinal purposes, they are offered for sale on local markets and herb-shops. However, because of the similar shape of the fleshy tuberous roots, the same vernacular names are often used for different species and even for representatives from other plant families. This uncertainty in purchasing appropriate plant material has already led to confusions in chemical and pharmaceutical literature (e.g., Shiengthong et al., 1974; Taguchi et al., 1977; Sekine et al., 1995). As shown in a recent report from our laboratory, striking chemical differences were already observed between *Stemona collinsae* Craib and *S. tuberosa* Lour. leading to completely different biological activities (Brem et al.,

* Corresponding author. Tel.: +43-1-4277-54070; fax: +43-1-4277-9541 (H. Greger); tel.: +43-1-4277-52107; fax: +43-1-4277-9521.
E-mail addresses: otmar.hofer@univie.ac.at (O. Hofer), harald.greger@univie.ac.at (H. Greger).
* Deceased.

0031-9422/03/$ - see front matter © 2003 Elsevier Ltd. All rights reserved.
doi:10.1016/S0031-9422(03)00332-7

2002). Thus, the usage of *Stemona* roots without preceding proper identification represents a serious risk for practical applications both in agriculture and medicine.

Based on properly identified and documented plant material from natural habitats a broad-based investigation on various *Stemona* species was carried out in our laboratory to demonstrate their different biogenetic capacities as well as biological activities against pathogenic fungi (Pacher et al., 2002) and herbivorous insects (Brem et al., 2002). In this connection we now have isolated and identified eight new alkaloids from four *Stemona* species, originating from different habitats in Thailand. Their structures were elucidated by means of ^{1}H, ^{13}C NMR and 2D methods including H/H-COSY, C/H-correlation, HMBC, and NOESY. Two key structures were also studied with X-ray diffraction. In addition, parallel bioassays against neonate larvae of the polyphagous pest insect *Spodoptera littoralis* Boisduval (Lepidoptera, Noctuidae), reared on artificial diet, were carried out to establish the insecticidal properties of the various components.

Since the structures of 56 already described *Stemona* alkaloids are mainly based on a pyrrolo[1,2-*a*]azepine nucleus (for recent reviews see Pilli and Ferreira de Oliviera, 2000; Xu, 2000), the discovery of a series of five novel pyrido[1,2-*a*]azepine derivatives deserves special interest. They mainly accumulate in *S. kerrii* Craib and were designated as stemokerrin (**1**), methoxystemokerrin-*N*-oxide (**2**), oxystemokerrin (**3**), oxystemokerrin-*N*-oxide (**4**), and pyridostemin (**5**) (Fig. 2). The structure of the major component, stemokerrin (**1**), was additionally determined by X-ray crystallography (Fig. 4). The remaining three new alkaloids were shown to be derived from the more widespread protostemonine (**6**) (Irie et al., 1970a; Ye et al., 1994) with a pyrrolo[1,2-*a*]azepine skeleton (Fig. 3) and were named dehydroprotostemonine (**7**), oxyprotostemonine (**8**), and stemocochinin (**9**). Whereas *S. kerrii* was characterized by a preponderance of pyrido[1,2-*a*]azepines, *S. curtisii* Hook.f. and *S. cochinchinensis* Gagnep. deviated by dominating pyrrolo[1,2-*a*]azepines, mainly accumulating stemofoline (**10**) (Irie et al., 1970b). The fourth species (HG 915), not identified in the present investigation, was mainly characterized by parvistemonine (**12**), previously isolated from *S. parviflora* C. H. Wright collected in Hainan island, China (Lin et al., 1990). As the correct taxonomic assignment of *Stemona* species in literature is encountering considerable difficulties, colour photographs were included from all four species investigated to facilitate their recognition (Fig. 1).

The present paper describes the isolation and structure elucidation of eight hitherto unknown *Stemona* alkaloids, their various distribution within four different species, as well as their insecticidal capacities in comparison to corresponding lipophilic crude extracts from various plant parts.

2. Results and discussion

2.1. Structure elucidation

On the basis of comparative HPLC, linked with UV diode-array detection, and parallel TLC, sprayed with chromogenic reagent, methanolic leaf and root extracts from four *Stemona* species were screened for characteristic alkaloids. Whereas ten compounds (**1**–**8**, **10**, **11**; Figs. 2 and 3) could readily be detected in HPLC profiles by their strong UV absorption at 296–312 nm ($MeOH/H_2O$), indicative of a conjugated dienone system, two (**9**, **12**) were only visible on TLC after spraying with Dragendorff reagent. As demonstrated in Table 3 their distribution in different species showed considerable variation. Nevertheless each species was clearly characterized by a single major component: Stemofoline (**10**), originally isolated from the stems and leaves of *S. japonica* (Irie et al., 1970b), was dominating in the roots of *S. curtisii* and *S. cochinchinensis* together with small quantities of the closely related 2′-hydroxystemofoline (**11**), recently reported for *S. collinsae* (Brem et al., 2002). Parvistemonine (**12**), previously described for the roots of *S. parviflora* (Lin et al., 1990), was shown to dominate in the unidentified species HG 915 from Northeast Thailand. In contrast, both provenances from *S. kerrii*, collected in North and Northwest Thailand, respectively, were characterized by a hitherto unknown alkaloid (**1**). The UV spectrum of **1** with a strong maximum at 306 nm ($MeOH/H_2O$) and IR with characteristic signals at 1758, 1682, and 1630 cm^{-1} (CCl_4) were indicative for an unsaturated lactone ring typical for most of the alkaloids isolated in the present investigation. However, on the basis of two-dimensional NMR analyses compound **1**, named stemokerrin, could be distinguished from all other major components by a different basic structure consisting of a pyrido- instead of a pyrroloazepine nucleus.

The chemical shifts of all ^{1}H and ^{13}C NMR resonances of the unsaturated lactonic 4-methoxy-3-methyl-2(5H)-furanone unit of **1** were almost identical with the same unit of many other *Stemona* alkaloids, e.g., **6**, **10**, and **11**. However, the remaining signals differed considerably from all other structural types known so far suggesting a new polycyclic core of the molecule. The H/H COSY connectivities of stemokerrin (**1**) ($[\alpha]_{20}^{D} = +136°$) showed two carbon chains, one consisting of CH_3-CH_2-CH-CH-CH_2-CH_2-CH_2-CH- and another starting with the N-CH_2 group, which was easily identified by the ^{1}H and ^{13}C chemical shifts using C/H correlation. This second chain N-CH_2-CH_2-CH = was characterized by an olefinic CH end group (^{1}H $\delta = 5.48$, ^{13}C $\delta = 100.2$ ppm, Table 1). The two chains corresponded to the sequences 3′-2′-1′-4-3-2-1-10a and 6-7-8. The resonance of 10-H, appearing as a broad singlet in the ^{1}H NMR, did not show any clear

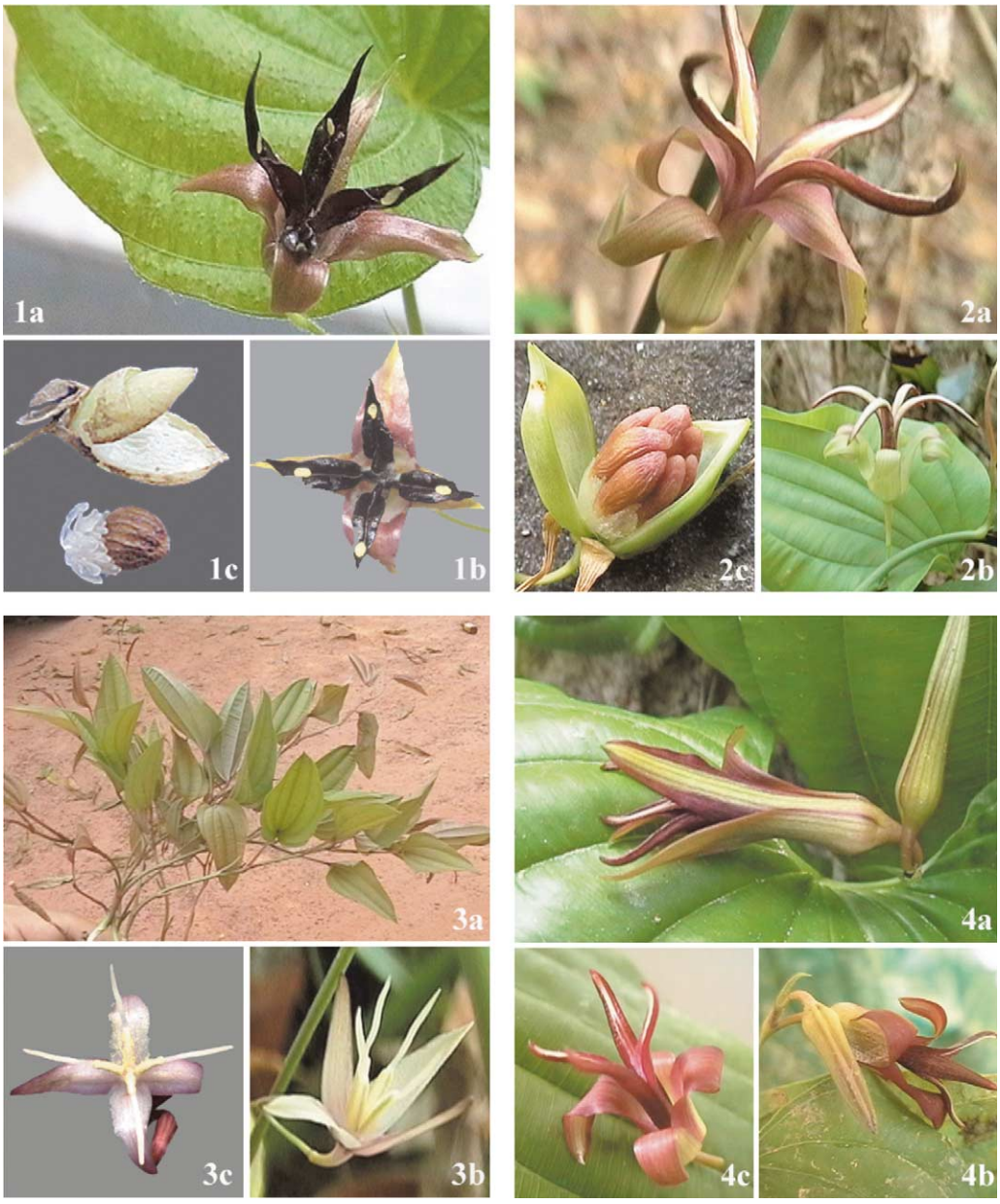

Fig. 1. Morphological characteristics of four *Stemona* species. (1) *S. kerrii* a, b flowers with four dark purple stamens containing yellow staminode-like appendices; c 1-seeded fruit with an aril consisting of many translucent appendices. (2) Unknown species HG 915 a, b flowers with different coloured tepals, c 8-seeded fruit. (3) *S. cochinchinensis* a habitus; b, c flowers with white to pinkish coloured tepals and narrow stamens. (4) *S. curtisii* a–c different views of flowers.

H/H-COSY cross peaks, therefore interrupting the corresponding chain. CH(11) and CH_3(18) showed again a direct coupling. However, close inspection of the HMBC long range C/H coupling data closed the gap between 10a and 11 and furnished informations for ring closures within the chains. The interactions from 8-H to C-9 and C10 as well as from 11-H to C-9, C-10a, and C-18 closed the connectivities within the azepine ring and the annelated oxygen containing five membered ring. The HMBC contacts from 18-H_3 to C-10, C-11, and C-12, from OCH_3 to C-14, and from 17-H_3 to C-14, C-15, C-16, and C-13 completed the linkage of the two five membered ring systems. The attachment of the nitrogen containing six membered ring including its conformation could be derived from the NOESY data and the coupling pattern of the ring protons. The axial orientations of protons 1a, 2a, and 3a were already clear from the three large coupling constants of the corresponding resonances (one geminal and two ax–ax couplings). The strong NOEs between the N-CH_2 protons (6-H_2) with H-1a and H-3a proved also the axial orientation of the CH_2(6) group attached to the N atom of the piperidine chair. Additionally, the strong NOE between 10a-H and 4-H proved an axial position for

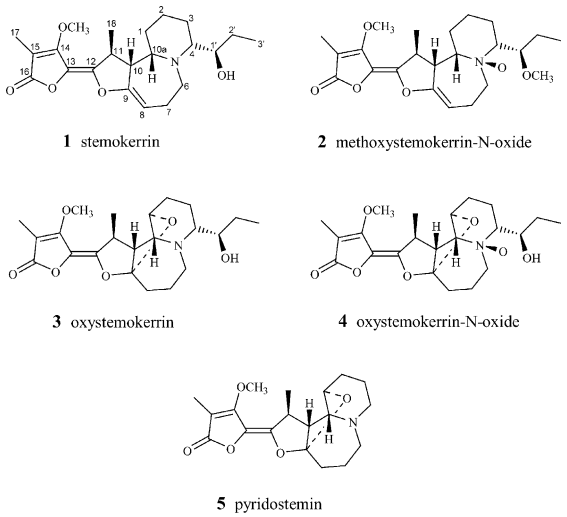

Fig. 2. Pyridoazepine alkaloids.

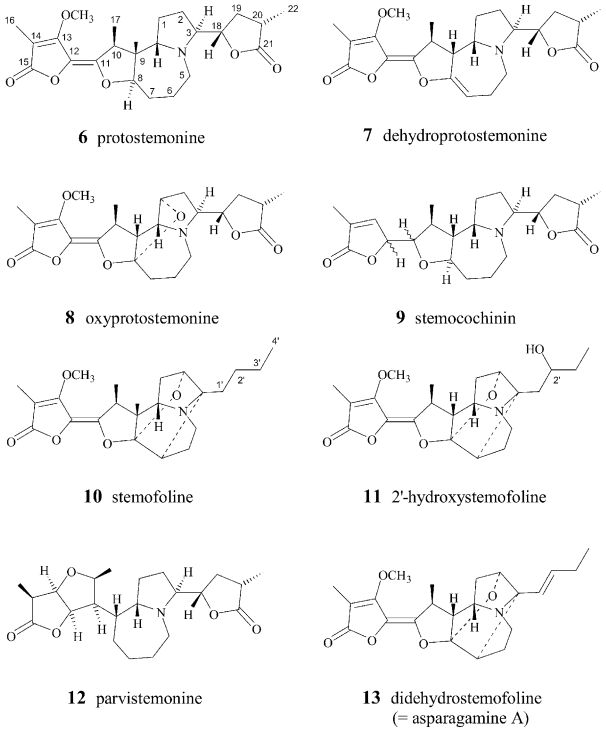

Fig. 3. Pyrroloazepine alkaloids.

these protons and consequently equatorial orientations for the C–C links 10a–10 within the azepine ring and 4-1′ of the side chain. The 1′-hydroxypropyl side group followed from the H/H-COSY connectivities, the NOESY cross peaks, and the chemical shifts including a complete analysis of the coupling constants within the chain (see Table 1). The derived structure was also compatible with the MS data with $m/z = 389$ for M^+ ($C_{22}H_{31}O_5N$, 8%), and a base peak of $m/z = 330$ after loss of the hydroxypropyl side chain (M^+-CH(OH)-CH_2-CH_3, 100%).

All these arguments concerning the conformation in solution agreed with the results of the X-ray crystallography (Fig. 4). The characteristics of the structure included a (*Z*) configuration of the C-12 = C-13 double bond (the two "ene-diolic" oxygen atoms of the two 5-rings in *syn* orientation) and a *cis* orientation of Me-18 and 10-H (also strong NOE 18-H_3↔10-H). These features were identical with many *Stemona* alkaloids of this type (e.g., compounds **6**–**8** and **10**, **11**). The absolute configurations of stemokerrin (**1**) shown in Fig. 4 was based on the absolute configurations of the closely related protostemonine chloroform solvate (**6**·$CHCl_3$, Fig. 5). In all known *Stemona* alkaloids the absolute configurations of the characteristic positions 10, 9, and 9a were identical. Since the tricyclic core of the new stemokerrin (**1**) is closely related to that of protostemonine (**6**) and the stemofolines (**10**, **11**), it is rather reasonable to correlate the absolute configurations of stemokerrin (**1**) via these compounds. It should be pointed out that the absolute configurations at C-3 in protostemonine (**6**) and at the "new" C-4 position in stemokerrin (**1**) are different, however, in both cases the relatively more stable equatorial positions are adopted (compare Figs. 4 and 5).

The X-ray derived conformations in the crystalline stemokerrin (**1**) matched perfectly the conformations derived by the NOESY cross peaks in solution. Consequently, the piperidine six membered ring is a chair and the azepine 7-ring annelated in *cis* configuration with C-6 standing axial and C-10 equatorial (Fig. 4). The 1′-hydroxypropyl side chain is orientated equatorially which agrees with the NOESY data discussed above. The absolute configuration at C-1′ is (*R*). Considering rotation about the 4-1′ bond, OH is in a *gauche* conformation relative to N allowing for a hydrogen bridge between O-H and the free e-pair of N. This conformation agrees also with NOESY peaks from 1′-H to 3a-H (ax) and 6-H_2 (C20-H to C7-Hax and C3-H_2 in Fig. 4). It is interesting to note that X-ray diffraction showed for C-3′ a disorder corresponding to a distribution over two sites. The conformation with C-3′ and the OH group in *anti* arrangement by rotation about the C-1′-C-2′ bond was populated 57% (C-3′ in Fig. 4), the remaining 43% showed C-3′ *anti* to C-4 and corresponds therefore to a zig-zag carbon chain (C-3″ in Fig. 4). Further details of this structure are given in the Experimental section.

All 2D derived connectivities for the new methoxystemokerrin-*N*-oxide (**2**) ($[\alpha]_{20}^{D} = +255°$) were completely identical with the data described for stemokerrin (**1**), differing only by a 1′-methoxy group in **2** replacing the 1′-hydroxy group in **1**. However, most chemical shift values were substancially different. Especially the ^{13}C resonances of the carbon atoms directly attached to N-5 showed strong downfield shifts of ca. 15 ppm (compare C-4, C-6, and C-10a in Table 1). The FAB HRMS

Table 1
^{1}H and ^{13}C NMR data of pyridoazepines **1**–**5** (**1**, **2**, and **5** in $CDCl_3$, **3** and **4** in CD_3OD)[a]

	^{1}H NMR					^{13}C NMR				
No.	**1**	**2**	**3**[b]	**4**[b]	**5**	**1**	**2**	**3**[b]	**4**[b]	**5**
1a	1.73 *dddd*	1.93 *m*[c]	4.03 *ddd*	4.38 br. *s*	4.00 *ddd*	16.9 *t*	23.8 *t*[c]	76.8 *d*	77.0 *d*	75.5 *d*
b	1.04 *dm*	1.72 *m*[c]								
2a	1.49 *m*	1.57 *m*[c]	1.81 *m*	2.02 *m*	1.62 *dddd*	24.8 *t*	23.3 *t*[c]	28.1 *t*	22.5 *t*	26.9 *t*
b	1.91 *dm*	1.65 *m*[c]	2.19 *m*	2.11 *m*	2.20 *ddm*					
3a	1.40 *dddd*	1.92 *m*[c]	1.64 *m*	1.98 *m*	1.82 *ddddd*	19.2 *t*	23.2 *t*[c]	30.8 *t*	23.0 *t*	18.8 *t*
b	1.25 *m*	1.72 *m*[c]	1.34 *m*	1.94 *m*	1.20 *ddddd*					
4a	2.60 *m*	3.26 *m*	2.59 *ddd*	3.31 *ddd*	2.98 *m*	69.9 *d*[c]	84.3 *d*	65.8 *d*	79.4 *d*	53.6 *t*
b					2.92 *m*					
6a	2.70 *ddd*	3.36 *ddd*	3.36 *m*	4.04 *m*	3.38 *ddd*	39.7 *t*	56.2 *t*	44.2 *t*	61.9 *t*	53.0 *t*
b	2.56 *m*	2.63 *ddd*	3.06 *ddd*	3.55 *ddd*	2.97 *m*					
7a	2.22 *m*	3.31 *m*	1.95 *m*	2.62 *m*	2.01 *m*	25.8 *t*	18.7 *t*	27.4 *t*	19.7 *t*	27.0 *t*
b	2.17 *m*	1.95 *m*	1.74 *m*	1.96 *m*	1.65 *m*					
8a	5.48 *ddd*	5.39 *ddd*	2.22 *m*	2.20 *m*	2.37 *ddd*	100.2 *d*	98.2 *d*	34.8 *t*	32.6 *t*	33.9 *t*
b			1.87 *m*	2.10 *m*	1.74 *ddd*					
9	–	–	–	–	–	157.4 *s*	157.9 *s*	121.8 *s*	154.1 *s*	120.5 *s*
10	3.15 br. *s*	4.53 br. *s*	2.88 *d*	3.38 *d*	2.66 *d*	52.8 *d*	44.2 *d*	57.4 *d*	52.3 *d*	57.1 *d*
10a	2.83 *dm*	3.21 *m*	3.50 br. *s*	3.93 br. *s*	3.42 *d*	62.4 *d*	78.5 *d*	66.4 *d*	85.4 *d*	62.0 *d*
11	2.92 *dq*	2.88 *dq*	3.20 *dq*	3.18 *dq*	3.06 *dq*	38.9 *d*	38.5 *d*	41.0 *d*	40.2 *d*	39.3 *d*
12	–	–	–	–	–	146.8 *s*	146.1 *s*	150.2 *s*	148.2 *s*	147.3 *s*
13	–	–	–	–	–	123.2 *s*	123.6 *s*	126.2 *s*	120.7 *s*	125.0 *s*
14	–	–	–	–	–	163.1 *s*	162.9 *s*	165.4 *s*	165.2 *s*	162.9 *s*
15	–	–	–	–	–	97.2 *s*	97.6 *s*	97.9 *s*	98.3 *s*	97.5 *s*
16	–	–	–	–	–	169.8 *s*	169.7 *s*	172.8 *s*	172.6 *s*	169.9 *s*
17	2.08 *s*	2.09 *s*	2.10 *s*	2.10 *s*	2.07 *s*	9.2 *q*	9.2 *q*	8.9 *q*	8.9 *q*	9.1 *q*
18	1.32 *d*	1.39 *d*	1.45 *d*	1.48 *d*	1.37 *d*	22.1 *q*	21.7 *q*	22.6 *q*	22.8 *q*	22.5 *q*
1′	3.40 *ddd*	4.13 *m*	3.59 *ddd*	4.08 *m*	–	70.1 *d*[c]	78.7 *d*	73.1 *d*	73.7 *d*	–
2′a	1.59 *ddq*	1.69 *m*	1.72 *ddq*	1.69 *m*	–	26.9 *t*	26.0 *t*	28.2 *t*	28.5 *t*	–
b	1.26 *m*	1.37 *m*	1.43 *ddq*	1.47 *m*						
3′	1.01 *t*	1.03 *t*	1.03 *t*	1.04 *t*	–	9.8 *q*	11.1 *q*	10.1 *q*	8.8 *q*	–
14-OMe	4.17 *s*	4.18 *s*	4.25	4.26 *s*	4.14 *s*	59.0 *q*	59.2 *q*	60.0 *q*	60.0 *q*	
19-OMe	–	3.50 *s*	–	–	–	–	57.9 *q*	–	–	–

[a] Coupling constants (*J*/Hz): **1**: 1a (13.2, 13.2, 13.2, 4.4), 1b (13.2), 2b (13.2), 3a (13.2, 13.2, 13.2, 4.2), 6a (12.5, 10.5, 1.5), 8 (9.0, 5.0, 2.0), 10 (appears as a broad s, all $J \leqslant 2$ Hz), 10a (12.5), 11 (2.0, 7.1), 18 (7.1), 1′ (9.8,8.3,2.7), 2′a (13.7, 2.7, 7.5), 2′b (13.7, 9.8, 7.5), 3′ (7.5); **2**: 6a (11.5, 11.5, <1), 6b (11.5, 5.1, <1), 8 (8.7, 4.7, 1.8), 11 (1.6, 7.1), 18 (7.1), 3′ (7.3); **3**: 1 (2.0, 1.0, 1.0), 4 (11.8, 9.0, 1.9), 6b (15.5, 11.5, ⩽1), 10 (4.8), 11 (4.8, 6.9), 18 (6.9), 1′ (9.0, 7.7, 3.1), 2′a (14.1, 3.1, 7.4), 2′b (14.1, 7.7, 7.4), 3′ (7.4); **4**: 4 (11.5, 9.0, 2.5), 6b (12.6, 6.5, <1), 10 (3.7), 11 (4.8, 6.8), 18 (6.8), 3′ (7.4); **5**: 1 (3.5, 2.0, 2.0), 2a (14.9, 13.1, 5.5, 3.5), 2b (14.9, 2.0), 3a (13.3, 13.3, 13.3, 4.5, 4.5), 3b (13.3, 7.5, 4.7, 2.1, <1), 6a (15.8, 12.6, <1), 8a (13.3, 5.3, 1.6), 8b (13.3, 12.0, 5.6), 10 (5.0), 10a (2.0), 11 (5.0, 6.9), 18 (6.9).

[b] All 2D assignments in CD_3OD; data in $CDCl_3$ are listed in the Experimental section.

[c] Exchangeable within the row.

showed a molecular ion of $m/z = 420.23805$ ($M^+ \cdot H$) which was compatible with a molecular formula of $C_{23}H_{33}O_6N$ for compound **2**. In the EIMS the molecular ion of $m/z = 419$ was rather weak (1%), the base peak at $m/z = 330$ (identical with the EIMS of **1**) corresponded to a loss of the side chain $CH(OCH_3)$-CH_2-CH_3 and an additional loss of an oxygen atom. A fragment with $m/z = 403$ corresponding to $M^+ - O$ was rather weak (2%) but clearly detectable. All NMR and MS data agreed with the presence of an additional oxygen attached to nitrogen N-5. A similar *N*-oxide has already been described for tuberostemonine (Lin and Fu, 1999).

The ^{1}H and ^{13}C NMR data of compound **3** ($[\alpha]_{20}^{D} = +289^\circ$), named oxystemokerrin, showed some similarities to the corresponding data of compound **1**, especially the unsaturated lactonic ring and the side chain. The most striking difference was the lack of any olefinic CH group in **3**. H/H-COSY revealed two continuous CH_n chains within the molecule, one starting at the terminal methyl group of the side chain: 3′-2′-1′-4-3-2-1-10a-10-11-18 and another one starting at N-CH_2: 6-7-8. The ring closure of the azepine 7-ring could be derived from HMBC long-range cross peaks from 10-H to the acetalic center C-9 and the methylene carbon C-8. Further important HMBC contacts include the interactions between 4-H and C-6 (6-H_2 to C-4 could be seen as well) linking the pyrido and the azepine ring systems and the contacts 18-H_3 to C-12 and 11-H to C-12 establishing the bridge to the unsaturated lactone ring. Position 1 showed chemical shifts typical for oxygen substitution (^{1}H $\delta = 4.03$ ppm, ^{13}C $\delta = 76.8$ ppm) and the quaternary C-9 was acetalic (^{13}C $\delta = 121.8$ ppm) imply-

Table 2
^{1}H and ^{13}C NMR data of pyrroloazepines **6–9** and **12** ($CDCl_3$)[a]

	^{1}H NMR					^{13}C NMR				
No.	**6**	**7**	**8**	**9**	**12**	**6**	**7**	**8**	**9**	**12**
1a	1.92 *m*	1.78 *m*	4.76 *ddd*	1.81 *m*	1.74 *m*	26.8 *t*	27.0 *t*	87.9 *d*	26.9 *t*[b]	26.7 *t*[b]
b	1.48 *m*	1.42 *m*		1.55 *m*	1.60 *m*					
2a	1.90 *m*	1.88 *m*	2.25 *m*	1.91 *m*	1.91 *m*	27.6 *t*	26.7 *t*	33.0 *t*[b]	27.0 *t*[b]	26.8 *t*[b]
b	1.46 *m*	1.38 *m*	1.74 *m*	1.37 *m*	1.49 *m*					
3	3.29 *ddd*	3.23 *ddd*	3.31 *ddd*	3.21 *ddd*	3.49 *m*	64.0 *t*	63.6 *d*	66.3 *d*	64.3 *d*	63.6 *d*
5a	3.48 *ddd*	3.37 *m*	3.08 *m*	3.44 *ddd*	3.41 *m*	46.4 *t*	43.8 *t*	50.8 *t*	47.4 *t*	46.3 *t*
b	2.93 *m*	3.34 *m*	2.97 *m*	2.88 *ddd*	2.90 *ddd*					
6a	1.64 *m*	2.56 *m*	1.70 *m*	1.54 *m*	1.71 *m*	20.2 *t*	22.6 *t*	20.8 *t*	20.2 *t*	24.6 *t*
b	1.51 *m*	2.10 *m*	1.44 *m*	1.37 *m*	1.51 *m*					
7a	2.37 *m*	5.24 *m*	2.25 *m*	2.06 *m*	1.76 *m*	34.2 *t*	99.7 *d*	32.4 *t*[b]	35.4 *t*	27.0 *t*[b]
b	1.50 *m*		1.74 *m*	1.27 *m*	1.45 *m*					
8	4.09 *ddd*	–	–	3.80 *m*	1.78 *m*	84.3 *d*	154.1 *s*	120.7 *s*	80.7 *d*	28.6 *t*
					1.43 *m*					
9	2.21 *ddd*	3.43 *m*	2.55 *d*	2.00 *m*	2.19 *m*	56.0 *d*	47.8 *d*	57.0 *d*	55.2 *d*	39.4 *d*
9a	3.73 *ddd*	3.74 *ddd*	3.60 *d*	3.64 *ddd*	3.44 *m*	58.5 *d*	65.1 *d*	69.8 *d*	59.0 *d*	62.8 *d*
10	2.91 *m*	2.99 *dq*	3.08 *m*	2.20 *m*	4.27 *dq*	39.5 *d*	37.7 *d*	39.6 *d*	39.6 *d*	77.3 *d*
11	–	–	–	3.77 *m*	2.07 *ddd*	149.2 *s*	145.8 *s*	146.7 *s*	83.4 *d*	49.9 *d*
12	–	–	–	4.90 *ddq*	5.04 *dd*	124.4 *s*	123.5 *s*	125.7 *s*	80.5 *d*	84.3 *d*
13	–	–	–	7.00 *dq*	4.33 *d*	163.2 *s*	163.1 *s*	162.9 *s*	146.2 *d*	84.0 *d*
14	–	–	–	–	2.74 *q*	97.0 *s*	97.1 *s*	97.6 *s*	131.0 *s*	44.8 *d*
15	–	–	–	–	–	170.1 *s*	169.9 *s*	169.8 *s*	174.4 *s*	179.6 *s*[c]
16	2.07 *s*	2.07 *s*	2.08 *s*	1.95 *dd*	1.29 *d*	9.2 *q*	9.1 *q*	9.1 *q*	10.9 *q*	14.9 *q*
17	1.34 *d*	1.31 *d*	1.37 *d*	1.08 *d*	1.21 *d*	20.8 *q*	22.4 *q*	22.0 *q*	15.9 *q*	19.3 *q*
18	4.16 *ddd*	4.10 *ddd*	4.23 *ddd*	4.14 *ddd*	4.21 *ddd*	83.5 *d*	84.3 *d*	82.3 *d*	84.0 *d*	83.1 *d*
19a	2.35 *ddd*	2.35 *ddd*	2.30 *ddd*	2.36 *ddd*	2.35 *ddd*	33.8 *t*	34.5 *t*	34.1 *t*	34.4 *t*	34.1 *t*
b	1.53 *m*	1.54 *ddd*	1.80 *m*	1.52 *ddd*	1.56 *ddd*					
20	2.60 *m*	2.60 *m*	2.68 *m*	2.60 *m*	2.60 *m*	34.9 *d*	35.0 *d*	35.9 *d*	35.0 *d*	34.9 *d*
21	–	–	–	–	–	179.5 *s*	179.5 *s*	179.3 *s*	179.6 *s*	179.5 *s*[c]
22	1.26 *d*	1.26 *d*	1.30 *d*	1.26 *d*	1.26 *d*	14.9 *q*	14.9 *q*	15.0 *q*	14.9 *q*	14.9 *q*
13-OMe	4.13 *s*	4.14 *s*	4.15 *s*	–	–	58.8 *q*	59.0 *q*	58.9 *q*	–	–

[a] Coupling constants (*J*/Hz): **6**: 3 (8.1, 7.0, 6.8), 5a (15.5, 4.6, <1), 8 (10.6, 10.2, 3.8), 9 (9.6, 8.8, 3.8), 9a (9.6, 5.8, 5.8), 17 (6.6), 18 (10.9, 7.0, 5.4), 19a (12.8, 8.1, 5.4), 22 (7.1); **7**: 3 (9.0, 8.0, 6.0), 9a (10.1, 4.9, 4.9), 10 (3.5, 7.1), 17 (7.1), 18 (11.2, 8.0, 5.3), 19a (12.6, 8.6, 5.3), 19b (12.6, 11.4, 11.2), 22 (7.1); **8**: 1 (2.3, 2.3, 2.3), 3 (9.3, 5.5, 4.0), 9 (5.3), 9a (2.0), 17 (7.0), 18 (9.7,5.6,4.1), 19a (12.4, 9.1,5.8), 22 (7.1); **9**: 3 (10.1, 7.7, 6.4), 5a (15.6, 5.3, ~1), 5b (15.6, 11.1, ~1), 9a (9.8, 4.9, 4.9), 12 (2.7, 2.7), 13 (2.7, 2.7), 16 (2.7, 2.7), 17 (6.6), 18 (11.2, 7.9, 5.3), 19a (12.6, 8.4, 5.3), 19b (12.6, 11.5, 11.2), 22 (7.1); **12**: 5b (15.4, 11.8, <1), 10 (7.3, 6.6), 11 (12.0, 7.3, 4.5), 12 (4.6, 4.5), 13 (4.6), 14 (8.1), 16 (8.1), 17 (6.6), 18 (11.5, 6.5, 5.5), 19a (12.6, 8.5, 5.5), 19b (12.6, 11.5, 11.5), 22 (7.1).

[b,c] Exchangeable within the row.

Table 3
Accumulation trends of pyrido- (**1–5**) and pyrroloazepine alkaloids (**6–12**) in leaves and roots of four *Stemona* species[a]

Species	Tissue	1	2	3	4	5	6	7	8	9	10	11	12
S. kerrii[b]	Leaves	+											
	Roots	●	+	○	+		+	○	+	+			
S. kerrii[c]	Leaves	No alkaloids detected											
	Roots	●	+		+		+	+		+			
S. curtisii	Leaves			+	+						+	+	
	roots			+			+	+	+	+	●	○	
S. cochinchinensis	Leaves										+	+	
	Roots						+			+	●	○	
S. sp. (HG 915)	Leaves			+	+	+							
	Roots			○		○							●

[a] Relative quantitities were determined on the basis of HPLC profiles by integration of corresponding peak areas. Major compounds (●), minor compounds (○), trace amounts (+).

[b] Collected in Doi Suthep near Chiang Mai.

[c] Collected in Khao Chomphu near Tak.

ing a possible oxygen bridge between C-1 and C-9. This 1–9 oxygen bridge is comparable to the 2–8 oxygen bridge typical for all stemofoline type alkaloids, e.g., compounds **10**, **11**. The assumption of this oxygen bridged structure is supported by mass spectral data: the molecular formula of $C_{22}H_{31}O_6N$ ($m/z = 405$ in the FD MS) showed a mass higher by 16 (1 oxygen atom) compared to **1** and the base peak is again characterized by the loss of the side chain $CH(OH)\text{-}CH_2\text{-}CH_3$ giving a fragment of $m/z = 346$. NOESY cross peaks from 1-H to 10a-H and 11-H confirmed the position of the oxygen bridge. Further important NOESY contacts between 4-H and 10a-H within the nitrogen containing six membered ring allowed to assign axial positions to these protons and therefore an equatorial position for the side chain attached at C-4. The NOESY cross peak 6-Ha to 1′-H was the same as for compound **1** and confirmed identical conformations and configurations of the side chain.

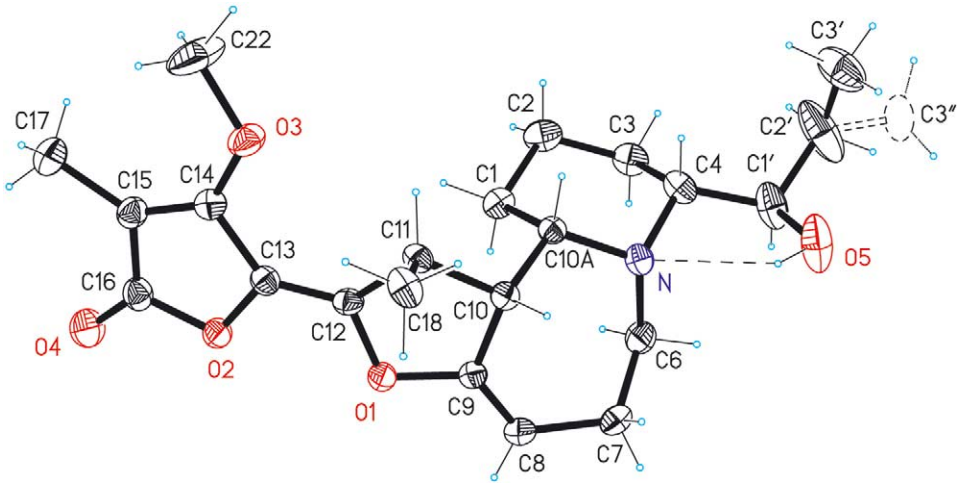

Fig. 4. Thermal ellipsoid plot of stemokerrin (**1**) in solid state showing the two conformations of the terminal methyl group of the side chain (C3′ and C3″) and the intramolecular O-H– – –N hydrogen bond, O(6)– – –N = 2.750(2) Å. C-atom designation corresponds with Fig. 2 and text.

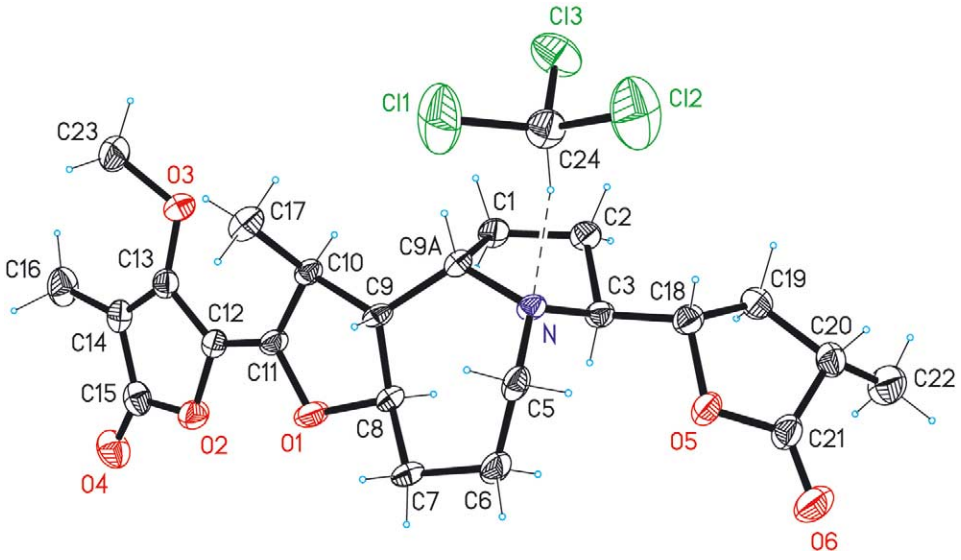

Fig. 5. Thermal ellipsoid plot of protostemonine chloroform solvate (**6**·$CHCl_3$) with its non-classical C-H– – –N hydrogen bond, C(24)– – –N = 3.380(6) Å. C-atom designation corresponds with Fig. 3 and text.

The 2D derived connectivities for compound **4** ($[\alpha]_{20}^{D} = +247°$) showed a completely identical pattern in comparison with compound **3**. However, the chemical shifts, especially for positions close to the nitrogen atom, were different. The mass of **4** was heavier by 16 compared to **3** with a small molecular ion at $m/z = 421$ (2%). A small peak at $m/z = 405$ after loss of an oxygen atom (5%), and the typical base peak at $m/z = 346$ after loss of oxygen and the side chain allowed the conclusion that compounds **3** and **4** differed only by oxygen substitution at the nitrogen atom. Compound **4** was therefore the *N*-oxide of **3**, named oxystemokerrin-*N*-oxide.

The ^{1}H and ^{13}C NMR data of compound **5** ($[\alpha]_{20}^{D} = +473°$) were very similar to that of **3**, but showed several characteristic deviations: all side chain resonances were missing, the CH(4) group had changed to a methylene group CH_2(4), and the ^{13}C resonances for C-3 and C-6 close to position 4 showed significantly different ^{13}C shift values compared to **3**. All assignments and connectivities were again confirmed by H/H COSY, HMQC, HMBC, and NOESY data, resulting in identical polycyclic systems for compounds **3** and **5**. Consequently compound **5**, named pyridostemin, simply lacks the C_3 side chain at position C-4. EIMS showed a molecular ion at $m/z = 347$ (100%!) and HRMS resulted in a molecular formula $C_{19}H_{25}NO_5$ confirming the NMR derived structure.

Protostemonine (**6**) is well described in literature (Ye et al., 1994), however, the ^{13}C NMR assignments of the methyl groups 16 and 17 should be mutually exchanged. We have obtained crystals of the chloroform solvate of **6** which were suited not only for the determination of

the molecular and solide state structure, but provided also the absolute configuration by X-ray analysis (Fig. 5). The compound **6**·$CHCl_3$ is remarkable in having a comparatively strong C-H– – –Cl hydrogen bond which makes this solvate stable under ambient conditions. Crystallographic data and selected bond lengths are given in the Experimental section. Further details have been deposited with the CCDC. First reports on the X-ray structures of protostemonine in the form of a methanol solvate and in the form of a methiodide (here with absolute configuration) have been given about thirty years ago (Ishizuka et al., 1972; Irie et al., 1973), however, except for unit cell data, no atomic parameters were given or deposited with the CCDC.

The new compounds **7**–**9** may be treated as closely related derivatives of protostemonine (**6**) and are discussed on the basis of this compound (Table 2, all assignments derived from extensive 2D measurements including H/H-COSY, HMBC, HMQC, and NOESY). The NMR data of compound **7** ($[\alpha]_{20}^{D} = +72^{\circ}$) deviated from the data of **6** by the absence of the methylene group CH_2(7) and the presence of a new olefinic methine group CH(7) (^{1}H $\delta = 5.24$ ppm, ^{13}C $\delta = 99.7$ ppm). The second carbon atom belonging to the new double bond was C-8, changing from CH to a quaternary C (^{13}C $\delta = 154.1$ ppm). Strong HMBC cross peaks from 10-H to the quaternary carbon atoms C-8, C-11, and C-12 confirmed the position of the newly introduced double bond. Compound **7** was therefore the 7,8-didehydro derivative of protostemonine (**6**) and was named dehydroprotostemonine. The MS data agreed with the proposed structure, giving a molecular ion $C_{23}H_{29}O_6N$ at $m/z = 415$ (14%) and a base peak for the fragment $m/z = 316$ (415−99) after loss of the lactone ring at C-3 (no. 18–22, $C_5H_7O_2$).

Compound **8** ($[\alpha]_{20}^{D} = +142^{\circ}$) showed an EIMS with a molecular ion $C_{23}H_{29}O_7N$ at $m/z = 431$ (9%) and a base peak at $m/z = 332$ (431−99) after loss of the $C_5H_7O_2$ lactone ring at C-3. This means that an additional oxygen atom is present in the polycyclic core of **8** in comparison with dehydroprotostemonine (**7**). Comparing the ^{1}H and ^{13}C NMR data (1D and 2D) of compounds **7** and **8**, the change of the olefinic resonances CH(7) and C(8) of **7** to a methylene group CH_2(7) and an oxygen bridge C(8)-O-CH(1) could be proved. This additional oxygen bridge forming the 5-ring 1-O-8-9-9a differed from the C(8)-O-CH(2) epoxy bridge forming a 6-ring which is characteristic for all stemofoline derivatives (compare **10**, **11**, and **13**). However, the oxygen substitution at position 1 followed clearly from the H/H-COSY cross peaks between 1-H and its direct neighbours (2-H_2 and 9a-H). The strong NOESY cross peaks between 1-H, 9a-H, and 9-H additionally proved the relative configurations shown in the formula scheme (oxygen bridge below the drawing plane). It should be noted that the oxygen bridge of compound **8**, named oxyprotostemonine, is fully comparable to the oxygen bridge in the pyridoazepines **3**–**5** where analoguously positioned bridgeheads are also leading to the closure of an additional 5-ring.

The most striking differences in the ^{1}H and ^{13}C NMR spectra of compound **9** ($[\alpha]_{20}^{D} = -52^{\circ}$) in comparison to all *Stemona* alkaloids with an unsaturated lactone ring were the lack of the 13-OCH_3 group and the appearance of three new CH groups in agreement with the lack of three quaternary C. This is especially clear in the ^{13}C NMR data (Table 2) showing on the one hand a very good agreement in comparison with protostemonine (**6**) but on the other hand a completely different pattern for the carbon atoms number 11–14 (8, 15, and 17 show also significantly different chemical shifts). All changes have occurred close to the unsaturated lactone ring, the other parts of **9** are identical with **6**. The coupling pattern of the chain 16-14-13-12-11 was rather clear and conclusive for the structure of this part of the molecule: CH_3(16) was a *dd* with two identical long range coupling constants of 1.7 Hz to 13-H and 12-H (appearing therefore as a triplet); 13-H was a *dq*, again with identical coupling constants of 1.7 Hz to 16-H_3 and 12-H (appearing therefore as a quintet); and 12-H was a *ddq*, again with the same coupling constants to 16-H3, 13-H, and 11-H (appearing therefore as a hexett). All available 2D cross peaks were also compatible with the structure of a demethyl-11,12-dihydroprotostemonine. The observed NOESY cross peaks from 11 to 10, 12, 13, 17, from 12 to 10, 11, 13, 17, and from 13 to 11, 12, 16 additionally supported this structure but did not allow an unambiguous decision concerning the stereochemistries at positions 11 and 12. The EIMS spectrum showed a molecular ion for $C_{22}H_{31}NO_5$ with $m/z = 389$ (3%), the base peak at $m/z = 292$ (389−97) can be easily explained by the loss of the unsaturated lactone ring ($C_5H_5O_2$), and a further prominent fragment could be found at $m/z = 290$ (389−99) corresponding to the usual base peak after loss of the saturated lactone ring ($C_5H_7O_2$). This fragmentation represented a further strong evidence for the structure of **9** as outlined above. The compound was designated as stemocochinine.

The stemofolines **10**, **11**, and **13** have already been described previously (Irie et al., 1970b; Jiwajinda et al., 2001; Brem et al., 2002). In the case of the known compound parvistemonine (**12**), the NMR data were given only for the hydrobromide salt (Lin et al., 1990). Therefore we have redetermined the structure of **12** by 1D and 2D NMR spectroscopy to obtain the relevant NMR data and assignments for the alkaloid in non-acidic solvent (Table 2).

2.2. Biogenetic connections

The co-occurrence of pyrido- and pyrroloazepine alkaloids in the same plant species (Table 3) suggested a

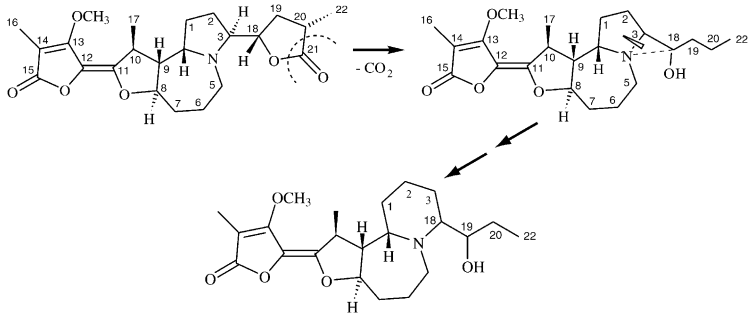

Fig. 6. Proposed biosynthetic connections between pyrrolo- and pyridoazepines.

common biogenetic origin (Fig. 6). Starting from the more widespread protostemonine (**6**), the butyl side chain at C-3, typical for the stemofolines (**10**, **11**, **13**), might be interpreted as the result of hydrolysis of the lactone ring followed by decarboxylation. The characteristic six-membered piperidine ring of the pyridoazepines most probably emerged from a five-membered pyrrolidine ring by ring cleavage and incorporation of C-18 from the butyl side chain (Fig. 6). The remaining propyl side chain is typical for the stemokerrins (**1**–**4**) and is missing in pyridostemin (**5**). With respect to the many *Stemona* alkaloids already known, it can be stated that the formation of the pyrroloazepine nucleus represents the basic structure of most derivatives. Apart from parvistemoamide, where an opening of the pyrroloazepine ring system led to a single ten-membered ring (Lin et al., 1991), only tuberostemoninol (Lin et al., 1994) and the isomeric neotuberostemoninol (Jiang et al., 2002) deviated by a different structure. They are also characterized by a pyridoazepine skeleton, however the six-membered piperidone ring arose in a different way: also starting from a pyrroloazepine precursor the structural transformation can be explained by opening C-1-C-9a and closing C-1-C-9.

Comparing the structures presented in the current paper it became apparent that the additional formation of an oxygen bridge represents an important structural feature for pyrrolo- and pyridoazepine alkaloids, hitherto only known from stemofolines (**10**, **11**, **13**). However, in contrast to the latter with an oxygen bridge between C-2 and C-8, all newly described pyrrolo- (**8**) and pyridoazepines (**3**–**5**) deviated with a bridge C-1-O-C-8 in the former, or C-1-O-C-9 in the latter derivatives. Obviously the analogue positions C-8 in pyrroloazepins and C-9 in pyridoazepins represent favoured positions for oxidation presumably also giving rise to the corresponding double bonds C-7=C-8 in dehydroprotostemonine (**7**), or C-8=C-9 in the stemokerrins (**1**, **2**), by dehydration. Moreover, the formation of *N*-oxides in **2** and **4** also represents a rare biogenetic step in this class of compounds, formerly only known from *N*-oxytuberostemonine (Lin et al., 1999).

2.3. Insecticidal activities

With respect to the insecticidal capacities of the crude extracts from the four different *Stemona* species investigated, *S. cochinchinensis* and *S. curtisii* clearly proved to be most active with LC_{50} values of 4 and 9 ppm (Table 4). As shown in Tables 3 and 5, this high activity can be attributed to the major compound stemofoline (**10**), already described for *S. collinsae* (Brem et al., 2002). In that report the potent insecticidal activity of stemofoline was assumed to be caused by neurotoxic interactions resulting in uncontrolled hyperactivity of larvae. In contrast to this excitatory effect causing immediate death of treated larvae, the extracts from *S. kerrii* and the unknown species HG 915 were characterized by a delayed entrance of death accompanied by softening of the larval bodies. In comparison with the stemofoline accumulating species, the two provenances of *S. kerrii* clearly showed less activity with LC_{50} values of 48 and 89 ppm, whereas the unknown species

Table 4
Acute (LC_{50}) and chronic (EC_{50}) toxicity of methanolic crude extracts from four *Stemona* species against neonate larvae of *Spodoptera littoralis*[a]

Plants	Tissue	LC_{50} (ppm)	EC_{50} (ppm)
S. kerrii[b]	Leaves	≫200	72
	Roots	48	12
S. kerrii [c]	Leaves	≫200	≫200
	Roots	89	23
S. curtisii	Leaves	≫100	65
	Roots	9	4
S. cochinchinensis	Leaves	36	30
	Roots	4	1
Stemona (HG 915)	Leaves	≫200	43
	Roots	≫175	22

[a] Neonate larvae ($n = 20$) were forced to feed on bean based artificial diet (3.8 g) spiked with various concentrations of the tested plant extracts. After 5 days of exposure, survival and weight of the surviving larvae were determined and compared to controls that had been exposed to solvent (MeOH) only. From the dose-response curves, LC_{50} and EC_{50} values were calculated by probit-log analysis.

[b] Collected in Doi Suthep near Chiang Mai.

[c] Collected in Khao Chomphu near Tak.

Table 5
Toxicity and growth inhibition of twelve *Stemona* alkaloids against neonate larvae of *Spodoptera littoralis* in comparison to the most active derivative didehydrostemofoline (**13**) isolated from *S. collinsae* (Brem et al., 2002)[a]

	LC_{50} (95% FL[b]) ppm	EC_{50} (95% FL[b]) ppm
Stemokerrin (**1**)	58 (48–73)	14.1 (12.0–16.4)
Methoxystemokerrin-*N*-oxide (**2**)	>100 (~150)	16.3 (10.0–27.3)
Oxystemokerrin (**3**)	5.9 (4.2–9.1)	0.7 (0.1–1.3)
Oxystemokerrin-*N*-oxide (**4**)	12.5 (7.2–22.5)	0.4 (0.1–0.9)
Pyridostemin (**5**)	149 (93–337)	96 (61–219)
Protostemonine (**6**)	17.7 (13.2–24.8)	2.2 (1.5–2.9)
Dehydroprotostemonine (**7**)	6.1 (4.3–9.1)	0.8 (0.4–1.3)
Oxyprotostemonine (**8**)	159 (99–839)	47 (30–75)
Stemocochinin (**9**)	170 (150–200)	61 (38–96)
Stemofoline (**10**)	2.0 (1.6–2.6)	1.5 (1.3–1.6)
2′-Hydroxystemofoline (**11**)	30 (27–35)	38 (7–182)
Parvistemonine (**12**)	≫200 (~350)	163 (133–234)
Didehydrostemofoline (**13**)	0.8 (0.7–1.1)	0.5 (0.3–0.6)

[a] Nonchoice feeding studies were conducted with neonate larvae of *Spodoptera littoralis* ($n=20$ for each treatment) that were released on artificial diet spiked with various concentrations of test compounds. After 5 days of exposure, survival and weight of the surviving larvae were determined and compared to controls that had been exposed to diet treated with solvent (MeOH) only. From the dose–response curves LC_{50} and EC_{50} values were calculated by probit-log analysis.
[b] Fiducial limits.

HG 915 even lacks acute toxicity at tested concentrations (Table 4). As shown in Table 4, leaf extracts were generally less toxic than the corresponding underground parts due to trace amounts of alkaloid derivatives (Table 3). As an exception, the leaf extracts of *S. cochinchinensis* were even more toxic ($LC_{50}=36$ ppm) than the roots of *S. kerrii* ($LC_{50}=48$ ppm) because of the presence of stemofoline (**10**).

In Table 5, insecticidal activities of 13 compounds were compared in order to highlight structure–activity relationships. With regard to the five novel pyrido[1,2-*a*]azepine derivatives, oxystemokerrin (**3**) with an oxygen bridge between the C-1 and C-8 of the pyridoazepine nucleus displayed the strongest activity with a LC_{50} value of 5.9 ppm. *N*-oxidation in **4** or insertion of a double bond in the azepine ring of **1** diminished activities to a LC_{50} value of 12.5 ppm in the former compound and 58 ppm in the latter. A significant decrease of toxicity, however, was caused by the loss of the open butyl side chain in **5** ($LC_{50}=149$ ppm) or its *O*-methylation in **2** ($LC_{50}>100$ ppm). Whereas insertion of a double bond in the azepine ring obviously reduced insect toxicity in pyridoazepines, an opposite effect was observed in the more common pyrroloazepine derivatives: the novel dehydroprotostemonine (**7**) with a double bond between C-7 and C-8 proved to be most active with a LC_{50} value of 6.1 ppm, whereas the corresponding saturated protostemonine (**6**) was less active with 17.7 ppm. Moreover, in contrast to the pyridoazepines the formation of an oxygen bridge in oxyprotostemonine (**8**) significantly reduced activity leading to a LC_{50} value of 159 ppm. Comparing the insecticidal activities of all alkaloids listed in Table 5 it became apparent, that the unsaturated lactonic 4-methoxy-3-methyl-2-furanone unit also plays a crucial role. It is modified or missing only in stemocochinin (**9**) and parvistemonine (**12**), where it led to a strong decrease of insecticidal activity with a LC_{50} value of 170 ppm for **9** or even more than 200 ppm for **12**, the major compound of the unknown species HG 915. As already reported previously, the striking differences between the three stemofoline derivatives **10**, **11**, and **13**, could be attributed to various transformations of the *n*-butyl side chain (Brem et al., 2002). Comparing the activities of the crude extracts with those of the corresponding major components (Tables 3–5), it became apparent that they were approximately as active as the isolated pure compounds. However, since equal amounts of crude extracts are usually less active than the isolated pure compounds, synergistic effects should be taken into consideration.

Generally, the *Stemona* alkaloids investigated in the present paper displayed two different modes of action: the stemofolines (**10**, **13**) were characterized by hyperactivity of larvae causing immediate death (Brem et al., 2002), whereas compounds **1**, **3**, **4**, **5**, **6**, **7**, and **8** led to paralysis and softening of the larval bodies, a phenomenon already described for stemospironine by Sakata et al. (1978). In that case however, larvae recovered completely when transposed to fresh diet and continued their development including normal oviposition.

3. Experimental

3.1. General

NMR: Bruker DRX400 WB. The spectra were referenced to the appropriate solvent signals ($CDCl_3$ ^1H δ 7.26; ^{13}C δ 77.0; MeOH-d_4 ^1H δ 3.35; ^{13}C δ 49.0). MS: Finnigan MAT 900 S. Optical rotation: Perkin-Elmer Polarimeter 241. IR: Perkin-Elmer 16PC FT-IR. HPLC: Hewlett Packard 1090 Series II, UV diode array detection at 280 nm, column 250×4.6 mm, Hypersil BDS C-18, 5 μm, mobile phase MeOH (gradient 60–100%) in aqueous buffer (0.01 M ammonium acetate, pH 7), flow rate 1 ml/min. X-ray: Bruker SMART CCD diffractometer.

3.2. Plant material

Four *Stemona* species were collected from different localities in Thailand: *S. kerrii* from a) North Thailand, Doi Suthep near Chiang Mai (HG 889); b) Northwest Thailand, Khao Chomphu near Tak (HG 892); *S. curtisii* from South Thailand, Ko Lipe near Ko Adang,

Satun Province (HG 865); *S. cochinchinensis* Gagnep. from Northeast Thailand, Phu Thok near Bung Kan, Nong Khai Province (HG 884); *Stemona sp.* from Northeast Thailand, Nong Wua So near Udon Thani (HG 915). Voucher specimens are deposited at the Herbarium of the Institute of Botany, University of Vienna (WU).

3.3. Extraction and isolation

Roots (including rhizomes) and leaves from different species were dried for 3–4 weeks, ground separately and extracted twice with MeOH at room temp for 5 days. Crude extracts were filtered and concd. The aqueous residues were extracted with $CHCl_3$ and the concentrated $CHCl_3$ fractions were used for comparative HPLC, TLC, and for preliminary insect bioassays. For preparative isolation lipophilic crude extracts were roughly sepd by column chromatography (Merck Silica gel 60, 0.2–0.5 mm) with hexane, EtOAc, and MeOH. Further separation of the alkaloid containing fractions was achieved by MPLC (400×40 mm column, Merck LiChroprep silica 60, 25–40 μm, UV detection 254 nm), with mixtures of MeOH in EtOAc as mobile phase. Preparative TLC (Merck, Silica gel F_{254} 60, 0.5 mm, 100% MeOH) on impregnated plates (0.1 M ammonium acetate, pH 7) was used to finally purify the alkaloids. Isolation and purification procedures of crude alkaloids were monitored by HPLC and analytical TLC (CH_2Cl_2–EtOAc–MeOH–diethylamine, 70–30–5–1) spraying with Dragendorff reagent.

Compounds **1**, **3**, **4**, **6**, **7**, **8** and **9** from 185 g roots of *S. kerrii* (HG 889). The $CHCl_3$ fraction (1054 mg) was roughly separated by column chromatography. The combined alkaloid containing fractions (400 mg) eluted with 25, 50, 75% MeOH in EtOAc, and 100% MeOH were further sepd by MPLC (100% EtOAc, and 15% MeOH in EtOAc). Fractions eluted with 100% EtOAc afforded 24 mg impure **6**, 12 mg impure **8**, and a mixture **3**, **7** and **9** (40 mg); those with 15% MeOH in EtOAc a mixture of **1** and **4** (50 mg). Whereas **6** was purified by cyclic MPLC (15% MeOH in EtOAc) to give 4 mg, further purification of compounds **8**, **3**, **7**, and **9**, as well as **1** and **4** was achieved by prep TLC (100% MeOH) to afford 2 mg pure **8**, 7 mg **3**, 11 mg **7**, 3 mg **9**, 16 mg **1**, and 6 mg **4**. 5 mg crystals of compound **1** were obtained from CH_2Cl_2/hexane.

Compound **2** from 94 g roots of *S. kerrii* (HG 892). The $CHCl_3$ extract (566 mg) was sepd by CC as mentioned above and the alkaloid containing CC fractions (212 mg) were further sepd by MPLC (100% EtOAc, 15%, and 30% MeOH in EtOAc). The fraction eluted with 15% MeOH gave a mixture of **1** and **9** (16 mg), and that with 30% MeOH 14 mg impure **2**. They were finally purified via prep TLC (100% MeOH) to yield 3 mg **2**, 5 mg **1**, and 1 mg **9**. Compounds **6** and **7** were identified by HPLC comparison with authentic samples.

Compounds **3**, **7**, **8**, **9**, **10**, and **11** from 736 g roots of *S. curtisii* (HG 865). CC of 1000 mg $CHCl_3$ extract led to 402 mg alkaloid containing fractions (50%, 75% MeOH in EtOAc, and 100% MeOH) which were further sepd by MPLC (15% MeOH in EtOAc) yielding 3 mg **8**, 93 mg **10**, and 16 mg **11** as pure compounds. Compounds **3**, **7**, and **9** were obtained as mixture (40 mg) which were further purified by prep TLC to give 13 mg **3**, 3 mg **7**, 4 mg **9**. Protostemonine (**6**) was identified by HPLC comparison.

Compounds **3**, **5**, and **12** from 209 g roots of *Stemona* spec. (HG 915). CC of 1700 mg $CHCl_3$ extract led to 417 mg alkaloid containing fractions (25, 50, 75% MeOH in EtOAc, and 100% MeOH) which were further sepd by MPLC (15% MeOH in EtOAc) leading to 19 mg **12** and a mixture of **3** and **12** (50 mg). Fractions with 30% MeOH in EtOAc afforded 27 mg impure **5**. The mixture **3** and **12** as well as **5** were finally sepd by prep TLC (100% MeOH) to give 13 mg **3**, 15 mg **12**, and 15 mg **5**.

Compounds **6**, **9**, **10**, and **11** from 477 g roots of *S. cochinchinensis* (HG 884). 1.3 g alkaloid containing CC fractions obtained from 2 g $CHCl_3$ extract were further sepd by MPLC as mentioned above to give 54 mg impure **11**, 245 mg impure **10**, 3 mg pure **9** and a mixture **6** and **11** (21 mg). Compounds **6** and **11** were sepd by prep TLC affording 2 mg **11** and **7** mg impure **6** from which 3 mg pure compound was obtained by crystallization in $CHCl_3$/hexane.

3.4. X-ray analyses

X-ray diffraction data were measured with a Bruker AXS SMART CCD platform 3-circle diffractometer and graphite monochromatized Mo-Kα radiation from a sealed X-ray tube. Data treatment and reduction was carried out with Bruker AXS programs and included semi-empirical corrections for absorption (Bruker AXS, 2001: programs SMART, version 5.054; SAINT, version 6.2.9; SADABS version 2.03; XPREP, version 5.1; SHELXTL, version 5.1. Bruker AXS Inc., Madison, WI, USA). The structures were solved with direct methods using program SHELXS97 and were refined by full-matrix least-squares on F^2 with program SHELXL97 (Sheldrick, 1997).

3.4.1. Crystal data for 1 (Fig. 4)

$C_{22}H_{31}NO_5$, $M=389.48$, monoclinic, space group $P2_1$ (no. 4), $a=8.917(2)$, $b=10.632(2)$, $c=11.775(3)$ Å, $\alpha=90°$, $\beta=105.74(1)°$, $\gamma=90°$, $V=1074.5(4)$ Å^3, $Z=2$, $D_c=1.204$ Mg/m^3, $T=213(2)$ K, $\mu=0.085$ mm^{-1}, $\lambda=0.71073$ Å, $F(000)=420$, colourless plate (0.18×0.18×0.04 mm) from CH_2Cl_2/hexane after intermediate formation of an unstable solvate. For data collection ω-scan frames (4×606 frames with $\Delta\omega=0.3°$, $t=25$ s; 2×909 + 600 frames with $\Delta\omega=0.2°$, $t=25$ s) were recorded to cover a complete sphere of the reciprocal space, $\theta_{max}=25°$, total reflections 18,143, unique reflec-

tions 3769, $R_{int} = 0.044$. Final refinement: data/restraints/parameters = 3769/1/270; $R_1 = 0.053$ (all data), $wR_2 = 0.087$ (all data). Absolute structure inferred from chemistry, optical rotation, and from the handedness of the structure of **6**·$CHCl_3$. Selected bond lengths (Å): O1-C12 1.381(2), O1-C9 1.397(2), O2-C16 1.386(2), O2-C13 1.390(2), O3-C14 1.340(3), O3-C22 1.437(3), O4-C16 1.209 (3), O5-C1′ 1.438(3), N-C6 1.485(3), N-C10A 1.487(2), N-C4 1.487(3), C1-C2 1.525(3), C1-C10A 1.528(3), C2-C3 1.526(3), C3-C4 1.525(3), C4-C1′ 1.528(3), C6-C7 1.525(3), C7-C8 1.511(3), C8-C9 1.310(3), C9-C10 1.504(3), C10-C10A 1.536(3), C10-C11 1.545(3), C11-C12 1.504(3), C11-C18 1.527(3), C12-C13 1.332(3), C13-C14 1.451(3), C14-C15 1.354(3), C15-C16 1.448(3), C15-C17 1.507(3), C1′-C2′ 1.501(4), C2′-C3′/C3″ 1.326(6)/1.275(10) (both values affected by disorder). CCDC 206104 (see below).

3.4.2. Crystal data for **6**·$CHCl_3$ (Fig. 5)

$C_{23}H_{31}NO_6$·$CHCl_3$, $M = 536.86$, orthorhombic, space group $P2_12_12_1$ (no.19), $a = 7.867(2)$, $b = 8.786(3)$, $c = 37.705(9)$ Å, $\alpha = \beta = \gamma = 90°$, $V = 2606.1(13)$ Å^3, $Z = 4$, $D_c = 1.368$ Mg/m^3, $T = 293(2)$ K, $\mu = 0.391$ mm^{-1}, $\lambda = 0.71073$ Å, $F(000) = 1128$, colourless plate (0.8×0.6×0.03 mm) from $CHCl_3$/hexane. For data collection 4×909 ω-scan frames ($\Delta\omega = 0.2°$, $t = 20$ s) were recorded to cover a complete sphere of the reciprocal space, $\theta_{max} = 25.03°$, total reflections 24,998, unique reflections 4392, $R_{int} = 0.066$. Final refinement: data/restraints/parameters = 4392/0/311; $R_1 = 0.081$ (all data), $wR_2 = 0.137$ (all data), absolute structure parameter 0.01(11). Selected bond lengths (Å): O1-C11 1.364(5), O1-C8 1.473(5), O2-C15 1.378(5), O2-C12 1.396(5), O3-C13 1.358(5), O3-C23 1.431(6), O4-C15 1.210(5), O5-C21 1.360(5), O5-C18 1.479(5), O6-C21 1.203(5), N-C5 1.475(5), N-C9A 1.480(5), N-C3 1.482(5), C1-C2 1.506(6), C1-C9A 1.554(5), C2-C3 1.533(5), C3-C18 1.512 (6), C5-C6 1.523(6), C6-C7 1.535(6), C7-C8 1.526(5), C8-C9 1.511(5), C9-C9A 1.531(5), C9-C10 1.544(5), C10-C11 1.506(5), C10-C17 1.517(6), C11-C12 1.363(5), C12-C13 1.447(6), C13-C14 1.343(6), C14-C15 1.468(6), C14-C16 1.508(6), C18-C19 1.547(6), C19-C20 1.534(6), C20-C21 1.487(6), C20-C22 1.507(7), C24-Cl1 1.705(5), C24-Cl2 1.738(5), C24-Cl3 1.754(5). CCDC 206105. (CCDC 206104-5 contain the supplementary crystallographic data for this paper. These data can be obtained free of charge via www.ccdc.cam.ac.uk/conts/retrieving.html or from the CCDC, 12 Union Road, Cambridge CB2 1EZ, UK; fax: +44 1223 336033; e-mail: deposit@ccdc.cam.ac.uk).

3.5. Stemokerrin. 4-Methoxy-3-methyl-5-[(2Z,11aS)-8t-((1R)-1-hydroxypropyl)-1c-methyl-(11ar,11bc)-1,2,5,6,8,9,10,11,11a,11b-decahydro-furo[3,2-c]pyrido[1,2-a]azepin-2-ylidene]-5H-furan-2-one (1)

Colourless plates, mp 138–141 °C; $[\alpha]_{20}^{D} = +136°$ (MeOH, $c = 0.3$). UV λ^{MeOH/H_2O} 306, 216 nm. IR ν^{CCl_4} cm^{-1} 3442 m, 2934 m, 2872 m, 1758 s, 1682 s, 1630 s, 1458 m, 1396 m, 1366 w, 1274 m, 1216 s, 1162 m, 1122 w, 1106 w, 1056 m, 1014 s, 972 w, 948 w, 938 w, 914 w, 670 w. ^{1}H and ^{13}C NMR see Table 1. EIMS (70 eV) m/z 389 (8, M$^+$), 360 (12, M$^+$ CH_3CH_2), 330 (100, M$^+$ $CH(OH)CH_2CH_3$), 315 (17), 122 (11), 83 (10). HREIMS m/z 389.2207 (calcd for $C_{22}H_{31}NO_5$, 389.2202).

3.6. Methoxystemokerrin-N-oxide. 4-Methoxy-3-methyl-5-[(2Z,11aS)-8t-((1R)-1-methoxypropyl)-1c-methyl-(11ar,11bc)-1,2,5,6,8,9,10,11,11a,11b-decahydro-furo[3,2-c]pyrido[1,2-a]azepin-2-ylidene]-5H-furan-2-one-N-oxide (2)

Amorphous, $[\alpha]_{20}^{D} = +255°$ (MeOH, $c = 0.2$). UV λ^{MeOH/H_2O} 308, 216 nm. IR ν^{CCl_4} cm^{-1} 2932 m, 2872 w, 1758 s, 1682 s, 1632 s, 1456 m, 1396 m, 1366 w, 1272 w, 1220 s, 1158 m, 1120 w, 1082 m, 1046 m, 1020 s, 1012 m, 972 w, 936 w, 904 w, 676 w. ^{1}H and ^{13}C NMR see Table 1. EIMS (70 eV) m/z 419 (1, M$^+$), 403 (2, M$^+$-oxygen), 401 (9), 346 (16), 330 (100, M$^+$-oxygen and -$CH(OCH_3)CH_2CH_3$), 328 (30), 172 (44), 156 (14), 83 (9), 57 (10). HRFABMS m/z 420.2381 (calcd for $C_{23}H_{33}NO_6$·H, 420.2386).

3.7. Oxystemokerrin. 4-Methoxy-3-methyl-5-[(2Z,11aS)-3at,11t-epoxy-8t-((1R)-1-hydroxypropyl)-1c-methyl-(11ar,11bc)-dodecahydro-furo[3,2-c]pyrido[1,2-a]azepin-2-ylidene]-5H-furan-2-one (3)

Amorphous, $[\alpha]_{20}^{D} = +289°$ (MeOH, $c = 0.4$). UV λ^{MeOH/H_2O} 298 nm. IR ν^{CCl_4} cm^{-1} 3486 w, 2952 m, 2874 w, 1756 s, 1694 m, 1628 s, 1458 m, 1396 m, 1366 m, 1282 w, 1230 w, 1216 m, 1154 m, 1108 w, 1090 w, 1042 m, 1026 s, 990 s, 954 w, 940 w, 916 w, 670 w. ^{1}H and ^{13}C NMR in CD_3OD see Table 1. ^{1}H NMR ($CDCl_3$) δ = 4.15 (*s*, 3H, OCH_3), 4.02 (narrow *m*, 1H, 1-H), 3.53 (br. *m*, 1H, 1′-H), 3.39 (br. *s*, 1H, 10a-H), 3.20 (br. *m*, 1H, 6a-H), 3.03 (br. *m*, 1H, 11-H), 2.94 (br. *t*, 1H, $J = \sim 15$ and ~ 12 Hz, 6b-H), 2.70 (*d*, 1H, $J = 5.0$ Hz, 10-H), 2.43 (*ddd*, 1H, $J = 12.0$, 9.0 and 2.0 Hz, 4-H), 2.28 (*m*, 1H, 8a-H), 2.23 (*m*, 1H, 2a-H), 2.08 (*s*, 3H, 17-H_3), 2.0-1.3 (*m*, 8H, 2b-H, 3a,b-H_2, 7a,b-H_2, 8b-H, and 2′a,b-H_2), 1.40 (*d*, 3H, $J = 7.0$ Hz, 18-H_3), 1.02 (*t*, 3H, $J = 7.4$ Hz, 3′-H_3). ^{13}C NMR ($CDCl_3$) δ = 169.9 (*s*, C-16), 162.9 (*s*, C-14), 119.9 (*s*, C-9), 97.5 (*s*, C-15), 75.0 (*d*, C-1), 70.5 (*d*, 1′-H), 65.8 (*d*, C-4), 58.9 (*q*, OCH_3), 56.5 (*d*, C-10), 42.8 (*t*, C-6), 39.7 (*d*, C-11), 26.9 (*t*, 2′-C), 22.5 (*q*, C-18), 9.6 (*q*, 3′-C), 9.1 (*q*, C-17), signals for the quaternary carbon atoms 2, 3, 7, 8, 10, 12, and 13 too weak for detection. EIMS (70 eV) m/z 405 (5, M$^+$), 376 (5, M$^+$-CH_3CH_2), 346 (100, M$^+$-$CH(OH)CH_2CH_3$), 288 (8), 149 (18), 59 (46). FDMS m/z 389 (100, M$^+$).

*3.8. Oxystemokerrin-N-oxide. 4-Methoxy-3-methyl-5-[(2Z,11aS)-3at,11t-epoxy-8t-((1R)-1-hydroxypropyl)-1c-methyl-(11ar,11bc)-dodecahydro-furo[3,2-c]pyrido[1,2-a]azepin-2-ylidene]-5H-furan-2-one-N-oxide (**4**)*

Amorphous, $[\alpha]_{20}^{D} = +247^{\circ}$ (MeOH, $c = 0.3$). UV λMeOH/H_2O 296 nm. IR ν^{CCl_4} cm^{-1} 2928 m, 2852 w, 1760 s, 1698 m, 1630 s, 1458 m, 1395 w, 1366 m, 1286 m, 1254 w, 1236 w, 1214 w, 1154 m, 1080 w, 1058 m, 1026 s, 1014 m, 978 m, 965 w, 946 w, 874 w. ^{1}H and ^{13}C NMR in CD_3OD see Table 1. ^{1}H NMR ($CDCl_3$) $\delta = 4.31$ (br.*s*, 1H, 1-H), 4.15 (*s*, 3H, OCH_3), 3.98 (*ddd*, 1H, $J = 9.6$, 7.1, 2.8 Hz, 1′-H), 3.90 (*ddd*, 1H, $J = 12.4$, 11.5, <1 Hz, 6a-H), 3.72 (br.*s*, 1H, 10a-H), 3.59 (*ddd*, 1H, $J = 12.4$, 6.5, <1 Hz, 6b-H), 3.48 (*d*, 1H, $J = 3.6$ Hz, 10-H), 3.13 (*ddd*, 1H, $J = 11.6$, 8.8, 2.8 Hz, 4-H), 2.92 (*dq*, 1H, $J = 4.1$, 7.1 Hz, 11-H), 2.69 (*m*, 1H, 7a-H), 2.20-1.80 (*m*, 7H, 2a,b-H_2, 3a,b-H_2, 7b-H, and 8a,b-H_2), 2.08 (*s*, 3H, 17-H_3), 1.63 (*m*, 1H, 2′a-H), 1.42 (*d*, 3H, $J = 7.1$ Hz, 18-H_3), 1.41 (*m*, 1H, 2′b-H), 1.01 (*t*, $J = 7.3$ Hz, 3′-H_3). ^{13}C NMR ($CDCl_3$) $\delta = 169.6$ (*s*, C-16), 162.6 (*s*, C-14), 155.6 (*s*, C-9), 162.6 (*s*, C-14), 146.7 (*s*, C-12), 119.2 (*s*, 13-H), 97.9 (*s*, 15-H), 84.8 (*d*, 10a-H), 77.9 (*d*, 4-H), 75.0 (*d*, C-1), 72.5 (*d*, 1′-H), 60.4 (*t*, C-6), 50.9 (*d*, C-10), 59.0 (*q*, OCH_3), 39.1 (*d*, 11-H), 22.2 and 22.0 (2×*t*, C-2 and C-3, exchangeable), 31.7 (*t*, C-8), 28.0 (*t*, C-2′), 22.5 (*q*, C-18), 18.6 (*t*, C-7), 9.1 (*q*, C-17), 8.5 (*q*, C-3′). EIMS (70 eV) *m*/*z* 421 (2, M^+), 405 (5, M^+-oxygen), 387 (9), 376 (6), 346 (100, M^+-oxygen and $M^-CH(OH)CH_2CH_3$), 204 (6), 164 (9), 167 (9), 69(7). FDMS *m*/*z* 421 (100, M^+).

*3.9. Pyridostemin. 4-Methoxy-3-methyl-5-[(2Z,11aS)-3at,11t-epoxy-1c-methyl-(11ar,11bc)-dodecahydro-furo[3,2-c]pyrido[1,2-a]azepin-2-ylidene]-5H-furan-2-one (**5**)*

Amorphous, $[\alpha]_{20}^{D} = +473^{\circ}$ (MeOH, $c = 0.4$). UV λ^{MeOH/H_2O} 298 nm. IR ν^{CCl_4} cm^{-1} 2946 m, 2870 w, 1756 s, 1694 m, 1628 s, 1456 m, 1446 w, 1396 m, 1364 m, 1342 w, 1316 w, 1298 w, 1282 w, 1270 w, 1254 w, 1224 m, 1216 m, 1156 m, 1062 m, 1045 m, 1024 s, 994 s, 950 m, 912 m, 880 w, 844 w, 682 w, 668 w, 618 w. ^{1}H and ^{13}C NMR see Table 1. EIMS (70 eV) *m*/*z* 347 (100, M^+), 220 (23), 193 (66), 192 (27), 137 (26), 122 (36), 96 (22). HREIMS *m*/*z* 347.1736 (calcd for $C_{19}H_{25}NO_5$, 347.1733).

*3.10. Protostemonine. 4-Methoxy-3-methyl-5-[(2Z,3aR)-1t-methyl-8t-((2S)-4c-methyl-5-oxo-tetrahydrofuran-2r-yl)-(3ar,10at,10bt)-decahydro-2H-furo[3,2-c]pyrrolo[1,2-a]azepin-2-ylidene]-5H-furan-2-one (**6**)*

(Irie et al., 1970a; Ye et al., 1994). UV λ^{MeOH/H_2O} 304 nm. IR ν^{CCl_4} cm^{-1} 2934 m, 2870 w, 1782 s, 1750 s, 1680 m, 1624 s, 1458 m, 1396 w, 1366 w, 1272 w, 1234 w, 1214 m, 1190 w, 1154 m, 1062 w, 1020 s, 960 w, 940 w, 674 w. ^{1}H and ^{13}C NMR see Table 2.

*3.11. Dehydroprotostemonine. 4-Methoxy-3-methyl-5-[(2Z,3aR)-1t-methyl-8t-((2S)-4c-methyl-5-oxo-tetrahydrofuran-2r-yl)-(3ar,10at,10bt)-1,1a,5,6,8,9,10,10a-octahydro-2H-furo[3,2-c]pyrrolo[1,2-a]azepin-2-ylidene]-5H-furan-2-one (**7**)*

Amorphous, $[\alpha]_{20}^{D} = +72^{\circ}$ (MeOH, $c = 0.3$). UV λ^{MeOH/H_2O} 312 nm. IR ν^{CHCl_3} cm^{-1} 2932 m, 2877 w, 1758 s, 1740 s, 1682 s, 1622 s, 1458 m, 1398 w, 1368 w, 1276 w, 1158 s, 1074 m, 1016 m, 960 w, 930 m, 850 w. ^{1}H and ^{13}C NMR see Table 2. EIMS (70 eV) *m*/*z* 415 (14, M^+), 337 (26), 316 (100, M^+-$C_5H_7O_2$), 292 (23), 260 (17), 233 (20), 83 (24). HREIMS *m*/*z* 415.1994 (calcd for $C_{23}H_{29}NO_6$, 415.1995).

*3.12. Oxyprotostemonine. 4-Methoxy-3-methyl-5-[(2Z,3aR)-3ac,10c-epoxy-1t-methyl-8t-((2S)-4c-methyl-5-oxo-tetrahydrofuran-2r-yl)-(3ar,10at,10bt)-decahydro-2H-furo[3,2-c]pyrrolo[1,2-a]azepin-2-ylidene]-5H-furan-2-one (**8**)*

Amorphous, $[\alpha]_{20}^{D} = +142^{\circ}$ (MeOH, $c = 0.2$). UV λ^{MeOH/H_2O} 298 nm. IR ν^{CCl_4} cm^{-1} 2930 m, 2874 w, 1777 s, 1756 s, 1694 w, 1628 s, 1458 m, 1449 w, 1396 w, 1366 m, 1282 w, 1230 w, 1216 w, 1156 m, 1060 w, 1040 m, 1028 m, 1002 s, 978 w, 928 w. ^{1}H and ^{13}C NMR see Table 2. EIMS (70 eV) *m*/*z* 431 (10, M^+), 332 (100, M^+-$C_5H_7O_2$), 222 (6), 150 (5), 69 (5). HREIMS *m*/*z* 431.1942 (calcd for $C_{23}H_{29}NO_7$, 431.1944).

*3.13. Stemocochinin. 3-Methyl-5-[(2Z,3aR)-1t-methyl-8t-((2S)-4c-methyl-5-oxo-tetrahydrofuran-2r-yl)-(3ar,10at,10bt)-decahydro-2H-furo[3,2-c]pyrrolo[1,2-a]azepin-2-yl]-5H-furan-2-one (**9**)*

Amorphous, $[\alpha]_{20}^{D} = -52^{\circ}$ (MeOH, $c = 0.2$). IR ν^{CCl_4} cm^{-1} 2930 m, 2874 w, 1776 s, 1454 m, 1380 w, 1356 w, 1290 w, 1186 w, 1174 w, 1150 m, 1112 w, 1074 m, 1048 w, 1016 m, 992 w, 924 w, 958 w. ^{1}H and ^{13}C NMR see Table 2. EIMS (70 eV) *m*/*z* 389 (3, M^+), 292 (100, M^+-$C_5H_5O_2$), 290 (86, M^+-$C_5H_7O_2$), 164 (10), 55 (13). FDMS *m*/*z* 389 (100, M^+).

*3.14. Parvistemonine. (3aR)-3t,5t-Dimethyl-tetrahydro-6t-[(9R)-3c-((2S)-4c-methyl-5-oxo-tetrahydrofuran-2r-yl)-(9r)-octahydro-1H-pyrrolo[1,2-a]azepin-9-yl]-(3ar,6ac)-3H-furo[3,2-b]furan-2-one (**12**)*

(Lin et al., 1990). IR ν^{CCl_4} cm^{-1} 2934 m, 2880 w, 1782 s, 1456 m, 1380 m, 1352 w, 1290 w, 1174 s, 1150 m, 1100 w, 1058 w, 1016 m, 940 w, 904 w. ^{1}H and ^{13}C NMR see Table 2.

3.15. Insect bioassays

Chronic feeding bioassays were carried out with neonate larvae of the polyphagous pest insect *Spodoptera littoralis* Boisduval (Lepidoptera, Noctuidae). The larvae were from a laboratory colony reared on artificial diet under controlled conditions at 26 °C as described previously (Srivastava and Proksch, 1991). Incorporation of crude extracts or compounds into artificial diet was performed according to standard procedures (Kubo, 1991). The test insects ($n = 20$) were kept on artificial diet spiked with 5 different concentrations of plant extracts (1–50 ppm: roots of *S. curtisii*, leaves and roots of *S. cochinchinensis*; 1–100 ppm: roots of *S. kerrii*; 10–200 ppm: leaves of *S. kerrii* and *S. curtisii*, leaves and roots of *Stemona* HG 915) or with eight different concentrations of pure alkaloids (0.5–70 ppm: **1**, **3**, **4**, **6**, **7**; 10–200 ppm: **2**, **8**, **12**), which were applicated with MeOH. Tests were conducted in duplicate (crude extracts) or in triplicate (pure compounds). Due to scarcity of material, **5** and **9** were tested only twice at four different concentrations ranging from 10 to 200 ppm. After 5 days (moist chamber, darkness, 26 °C) the survival rate and the larval growth of the surviving larvae were monitored in comparison to controls that had been exposed to diet treated with solvent only. From the dose-response curves LC_{50} and EC_{50} values were calculated by probit-log analysis (Norusis, 1999).

Acknowledgements

We are grateful to Professor K. H. Ongania, Institute of Organic Chemistry, University of Innsbruck, Austria for mass spectra and Dr. Suyanee Vessabutr, Technical and Research Department, Queen Sirikit Botanic Garden, Chiang Mai, Thailand, for her valuable help in collecting plants. We also thank Anton Siedler from the Botanical Garden, University of Vienna, for providing photographs. This work was supported by the Austrian National Committee for the Intergovernmental Program "Man and Biosphere".

References

Brem, B., Seger, C., Pacher, T., Hofer, O., Vajrodaya, S., Greger, H., 2002. Feeding deterrence and contact toxicity of *Stemona* alkaloids—a source of potent natural insecticides. Journal of Agricultural and Food Chemistry 50, 6383–6388.

Duyfjes, B.E.E., 1993. Stemonaceae. Flora Malesiana Ser. I, 11, 399–409.

Irie, H., Harada, H., Ohno, K., Mizutani, T., Uyeo, S., 1970a. The structure of the alkaloid protostemonine. Chemical Communications, 268–269.

Irie, H., Masaki, N., Ohno, K., Osaki, K., Taga, T., Uyeo, S., 1970b. The crystal structure of a new alkaloid, stemofoline, from *Stemona japonica*. Chemical Communications, 1066.

Irie, H., Ohno, K., Osaki, K., Taga, T., Uyeo, S., 1973. X-ray crystallographic determination of the structure of the alkaloid protostemonine. Chemical and Pharmaceutical Bulletin 21, 451–452.

Ishizuka, K., Ohno, K., Taga, T., Masaki, N., 1972. The crystal structures of protostemonine methanol solvate and protostemonine methiodide. Acta Crystallographica A28, Part S4–S20, II-26. (congress abstract).

Jiang, R.W., Hon, P.M., But, P.P.H., Chung, H.S., Lin, G., Ye, W.C., Mak, T.C.W., 2002. Isolation and stereochemistry of two new alkaloids from *Stemona tuberosa*. Tetrahedron 58, 6705–6712.

Jiwajinda, S., Hirai, N., Watanabe, K., Santisopasri, V., Chuengsamarnyart, N., Koshimizu, K., Ohigashi, H., 2001. Occurrence of the insecticidal 16,17-didehydro-16(*E*)-stemofoline in *Stemona collinsae*. Phytochemistry 56, 693–695.

Kubo, I., 1991. Screening techniques for plant–insect interactions. In: Dey, P.M., Harborne, J.B., Hostettmann, K. (Eds.), Insect–Plant Interactions. Springer-Verlag, Berlin, pp. 95–120.

Lin, W.H., Yin, B.P., Tang, Z.J., Xu, R.S., Zhong, Q.X., 1990. The structure of parvistemonine. Acta Chimica Sinica 48, 811–814.

Lin, W.H., Xu, R.S., Zhong, Q.X., 1991. Chemical studies on *Stemona* alkaloids I. Studies on new alkaloids of *Stemona parviflora* C. H. Wright. Acta Chimica Sinica 49, 927–931.

Lin, W.H., Ma, L., Cai, M.S., Barnes, R.A., 1994. Two minor alkaloids from roots of *Stemona tuberosa*. Phytochemistry 36, 1333–1335.

Lin, W.H., Fu, H.Z., 1999. Three new alkaloids from the roots of *Stemona tuberosa*. Journal of Chinese Pharmaceutical Sciences 8, 1–7.

Norusis, M. J., 1999. SPSS Advanced Models 9.0. SPSS Inc. Chicago, IL.

Pacher, T., Seger, C., Engelmeier, D., Vajrodaya, S., Hofer, O., Greger, H., 2002. Antifungal stilbenoids from *Stemona collinsae*. Journal of Natural Products 65, 820–827.

Pilli, R.A., Ferreira de Oliveira, M.C., 2000. Recent progress in the chemistry of the *Stemona* alkaloids. Natural Product Reports 17, 117–127.

Sakata, K., Aoki, K., Chang, C.F., Sakurai, A., Tamura, S., Murakoshi, S., 1978. Stemospironine, a new insecticidal alkaloid of *Stemona japonica* Miq. Isolation, structural determination and activity. Agricultural and Biological Chemistry 42, 457–463.

Sekine, T., Ikegami, F., Fukasawa, N., Kashiwagi, Y., Aizawa, T., Fujii, Y., Ruangrungsi, N., Murakoshi, I., 1995. Structure and relative stereochemistry of a new polycyclic alkaloid, asparagamine A, showing anti-oxytocin activity, isolated from *Asparagus racemosus*. Journal of the Chemical Society, Perkin Transactions I, 391–393.

Sheldrick, G.M., 1997. SHELX97. Program System for Crystal Structure Determination. University of Göttingen, Germany.

Shiengthong, D., Donavanik, T., Uaprasert, V., Roengsumran, S., Massy-Westropp, R.A., 1974. Constituents of Thai medicinal plants III. New rotenoid compounds—stemonacetal, stemonal, and stemonone. Tetrahedron Letters 2015–2018.

Srivastava, R.P., Proksch, P., 1991. Kontakttoxizität und Fraßhemmung von Chromenen aus Asteraceae gegenüber *Spodoptera littoralis* (Lepidoptera: Noctuidae). Entomologia Generalis 15, 265–274.

Taguchi, H., Kanchanapee, P., Amatayakul, T., 1977. The constituents of *Clitoria macrophylla* Wall. Cat., a Thai medicinal plant. The structure of a new rotenoid, clitoriacetal. Chemical and Pharmaceutical Bulletin 25, 1026–1030.

Tsi, Z.H., Duyfjes, B.E.E., 2000. Stemonaceae. In: Wu, Z.Y., Raven, P. (Eds.), Flora of China, Vol. 24. Science Press, Beijing, pp. 70–72.

Xu, R.S., 2000. Some bioactive natural products from Chinese medicinal plants. In: Atta-ur-Rahman (Ed.), Studies in Natural Products Chemistry, Vol. 21. Elsevier, Amsterdam, pp. 729–772.

Ye, Y., Qin, G.W., Xu, R.S., 1994. Alkaloids of *Stemona japonica*. Phytochemistry 37, 1205–1208.